High Performance Fringe-Field Switching with a Negative Dielectric Anisotropy Liquid Crystal

Yuan Chen, Zhenyue Luo, Fenglin Peng and Shin-Tson Wu
College of Optics and Photonics, University of Central Florida, Orlando, Florida 32816, USA

Abstract
Using our new negative Δε LC material in a fringing field switching (n-FFS) cell, we demonstrated superior performances to conventional positive Δε FFS (p-FFS) LCD in transmittance, viewing angle, cell gap sensitivity, gamma curve, while keeping a comparable operation voltage and response time. Therefore, n-FFS has potential to replace p-FFS for next-generation mobile displays.

Author Keywords
Fringe-field switching; liquid crystal display

1. Introduction
Fringe field switching (FFS) LCDs [1-5] have been widely used in smartphones and tablet computers. Presently, most FFS displays use positive dielectric anisotropy ($\Delta\varepsilon$) LCs. The primary reason is that it is relatively easy to obtain nematic LCs with a large Δε (~10) while keeping a low viscosity. Large Δε helps to reduce operation voltage while low viscosity helps to achieve fast response time. However, positive LC-based FFS (p-FFS) displays exhibit some problems: 1) its peak transmittance is limited to ~88%; 2) the voltage-dependent transmittance (VT) curves do not overlap well for RGB colors. Thus, three gamma curves are required, which increases the complexity of driving electronics; and 3) a small but noticeable image flickering due to flexoelectric effect exists.

To overcome these problems, here we report a FFS mode using a negative $\Delta\varepsilon$ LC, designated as n-FFS. Our n-FFS exhibits some outstanding features: 1) high transmittance (98%), 2) single gamma curve for RGB pixels, 3) both on-state voltage and peak transmittance are relatively insensitive to cell gap variation, 4) slightly wider viewing angle, 5) faster response time due to slightly thinner cell gap, and 6) comparable on-state voltage to p-FFS although negative LCs usually have a smaller $\Delta\varepsilon$ than their positive counterparts. Therefore, n-FFS has potential to replace p-FFS for next-generation mobile displays.

2. Experiment
In experiment, we prepared a negative LC mixture (UCF-N1) with Δn~0.116 at λ=633nm and relatively low viscosity. The main compositions of UCF-N1 are lateral difluoro biphenyl and cyclohexane-biphenyl compounds [6]. For benchmarking, we compare our results with a low viscosity commercial LC mixture (Merck MLC-6882) whose physical properties are listed in Table I. For comparison purpose, we assume UCF-P1 has $\Delta\varepsilon$=10 while other properties remain the same as UCF-N1.

To investigate the electro-optical performances at different wavelength, we measured the birefringence dispersion for MLC-6882 and UCF-N1 and fit the results [7] using single-band birefringence dispersion model [8]:

$$\Delta n = G\lambda^2\lambda^{*2}/(\lambda^2-\lambda^{*2}), \quad (1)$$

where λ^* is the average resonance wavelength of the LC and G is a proportionality constant. Through fitting, we obtained G=2.82 μm^{-2}, λ^*=177.5 nm and G=2.10 μm^{-2}, λ^*=218.4 nm for MLC-6682 and UCF-N1, respectively. With a higher Δn, UCF-N1 has a longer resonance wavelength as expected. With these fitting parameters, the birefringence at a desired wavelength can be calculated through Eq. (1). For instance, at λ=550 nm, Δn=0.119 and 0.0983 for UCF-N1 and MLC-6882, respectively.

Table I. Physical properties of the LCs studied. (Data were measured at 23˚C, λ=633nm and 1kHz)

Mixture	T_c(˚C)	Δn	γ_1 (mPa.s)	Δε
MLC-6882	69.0	0.097	108	-3.1
UCF-N1	73.3	0.116	123	-3.82
UCF-P1	73.3	0.116	123	10

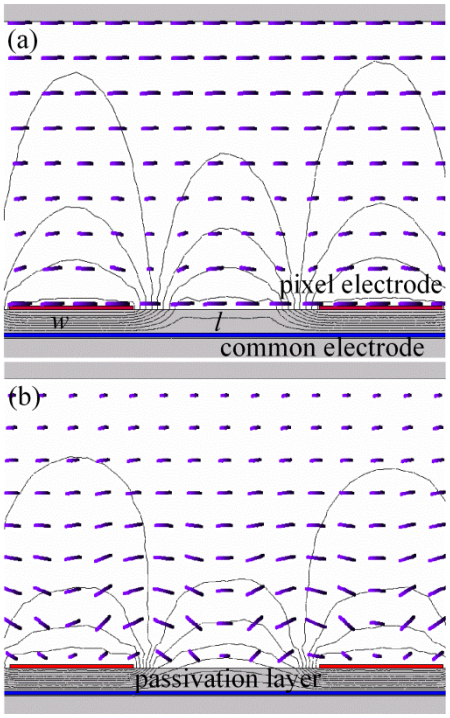

Figure 1. Device configuration of FFS structure, equal-potential lines, and LC director deformation of (a) n-FFS and (b) p-FFS.

3. Results and Discussion
The electro-optical properties of both n-FFS and p-FFS are calculated by a commercial LCD simulator DIMOS.2D and the extended Jones matrix [9, 10]. As will be shown later, the preferred $d\Delta n$ value for achieving high transmittance at λ=550 nm

 ISSN 0097-966X/13/4401-0334-$1.00 © 2013 SID

and fast response time is ~360 nm for n-FFS and ~380 nm for p-FFS. This difference results from the more efficient LC director reorientation in the n-FFS. To make a fair comparison between n-FFS and p-FFS, we use the same electrode width w=2 μm and gap l=3 μm, same pretilt angle (2°) but the rubbing angle is 10° and 80° respectively with respect to the horizontal axis. Figures 1(a)

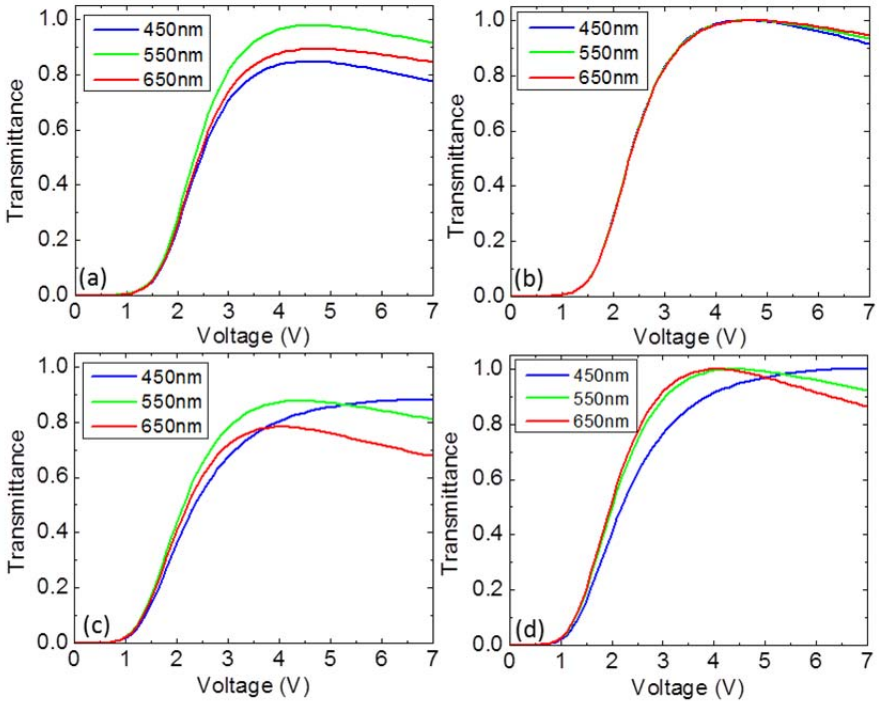

Figure 2. VT curves for (a) FFS-N1 and (c) FFS-P1; Normalized VT curves for (b) FFS-N1 and (d) FFS-P1

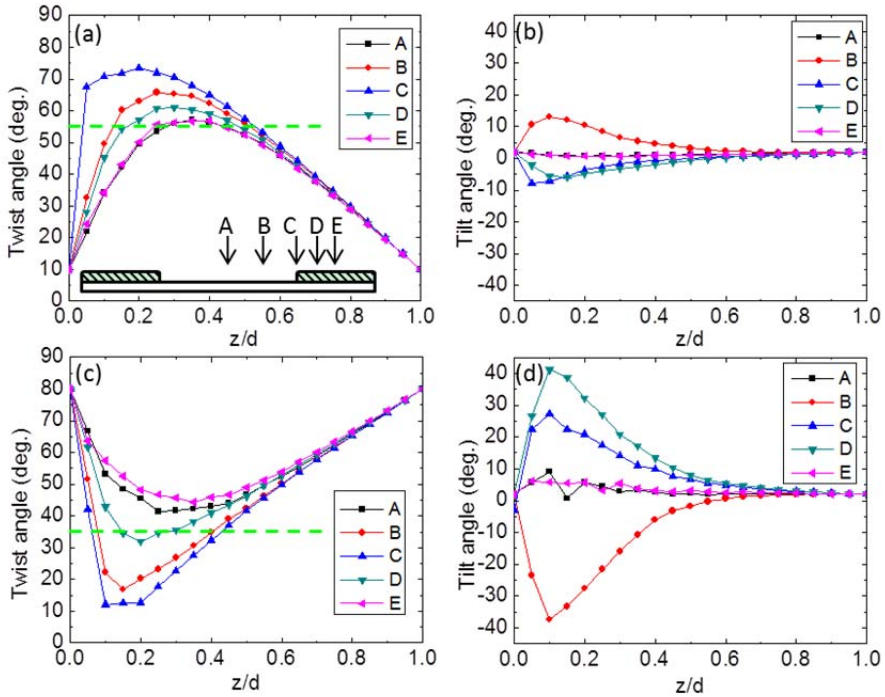

Figure 3. Twist angle distribution of (a) FFS-N1 and (c) FFS-P1; Tilt angle distribution of (b) FFS-N1 and (d) FFS-P1.

and 1(b) show the device configuration, calculated equal-potential lines and LC director deformation in a voltage-on state. The passivation layer between the pixel and common electrodes is SiO_x [11] whose thickness is d_p=250 nm and dielectric constant is ε_p=4.5. The cell is sandwiched between two crossed linear polarizers, and the transmission axis of the bottom polarizer is parallel to the rubbing direction.

3.1. VT Curves

Figure 2(a) depicts the simulated VT curves for n-FFS using UCF-N1 with d=3.02 μm. For convenience, let us call it FFS-N1. The peak transmittance (T_p) of FFS-N1 reaches ~98% (λ=550 nm) at the on-state voltage V_{on}=4.6V. Moreover, both RGB colors have nearly the same V_{on}. Figure 2(b) depicts the normalized VT curves and they overlap amazingly well. Thus, a single gamma curve driving can be realized for n-FFS, which would simplify the driving circuit.

For comparison, we also calculate the VT curves of a p-FFS cell (d=3.19μm) using UCF-P1. Let us call it FFS-P1. Results are shown in Fig. 2(c). The dispersion of VT curves for RGB colors is quite noticeable. At 550nm, T_p reaches ~88% at V_{on}=4.4V. The V_{on} for 650nm is 4.0V and T_p=78.3%. For λ=450nm, the peak transmittance can reach 88.1%, but at a much higher voltage (6.8V). Figure 2(d) depicts the normalized VT curves. Obviously, they do not overlap well. Thus, three different gamma curves are needed to drive the RGB pixels.

3.2. Director Deformation Distribution

In order to better understand the transmittance and gamma curve differences, we investigate the LC twist and tilt angle distributions [11-14] for both FFS-N1 and FFS-P1 at five positions (A to E as Fig. 3(a) shows). A twist angle of 45˚ would induce the maximal phase retardation. From Fig. 3, the LC molecules are twisted near the bottom of the cell (0.2<z/d<0.4) by the electric field and gradually reoriented back to the rubbing direction due to the anchoring force provided by the top surface. For FFS-N1, the maximal twist angle from the initial rubbing direction is around 46º at A and E. The tilt angle at A and E is close to 0, which would contribute effectively to the phase retardation. At B, C, and D, the horizontal electric field is stronger and the maximal twist angle is ~55º. Meanwhile, the tilt angle at z/d~0.1 is ~±10º, which would slightly decrease the phase retardation and compensate the over twist. Moreover, the on-state n-FFS cell is like two TN cells [11] due to the small tilt angle. As a result, polarization rotation effect dominates and the color dispersion is negligible. On the contrary, the maximal twist angle of FFS-P1 is either larger than 63º (B and C) or smaller than 38º (A and E). The over- or under-twist leads to inefficient phase retardation. Only at position D, the maximal twist angle is about 48º, however the tilt angle is about 41º at z/d=0.1. The large tilt angle caused by the strong vertical field dramatically decreases the effective birefringence and hence the transmittance. Meanwhile, with large tilt angle at positions B, C, and D, the phase retardation effect (which is wavelength sensitive) becomes quite obvious, resulting in severe wavelength dispersion. The splay deformation occurs and electric polarization is induced, which is known as flexoelectric effect [15]. Light transmittance differs from negative to positive frames, resulting in a small image flickering. On the contrary, this effect is negligible in n-FFS due to the small tilt angle.

Moreover, the reduced effective birefringence and the decreased twisting torque due to the large tilt require a higher voltage to achieve the peak transmittance. Therefore, FFS-P1 has a comparable V_{on} (4.4V) to FFS-N1 (4.6V), although the $\Delta\varepsilon$ of UCF-P1 is +10, which is much larger than that of UCF-N1 (-3.82). Thinner passivation layer thickness or larger dielectric constant passivation layer could further reduce the driving voltage because of less voltage shielding effect [16].

3.3. Response Time

Both rise time and decay time are calculated between the 10% and 90% transmittance and results are shown in Table II. The p-FFS cell is expected to have faster response time because it is easier to obtain large $\Delta\varepsilon$ and low viscosity at the same time. For the n-FFS cell with MLC-6882 (d=3.66μm), the rise time is 23.4ms and decay time is 34.8ms. However, with the development of low γ_1 and high Δn negative $\Delta\varepsilon$ LC, such as UCF-N1, the response time can be greatly improved. The calculated rise time is 16.2ms and the decay time is 24.1ms for FFS-N1. If we further assume UCF-P1 has the same rotational viscosity (123 mPas) and same birefringence (Δn=0.116) as UCF-N1 but $\Delta\varepsilon$=10, from simulation we find that FFS-P1 has slower rise time (23.8ms) and decay time (25.7ms) than FFS-N1 because of larger molecular tilt angle and slightly thicker cell gap.

Table II. Simulated response time for the three LCs studied.

Mixture	d(μm)	V_{on} (V)	T_p (%)	Rise time (ms)	Decay time (ms)
MLC-6882	3.66	4.5	98.7	23.4	34.8
UCF-N1	3.02	4.6	97.8	16.2	24.1
UCF-P1	3.19	4.4	87.7	23.8	25.7

3.4. Cell Gap Effect

The cell gap or phase retardation effect on the peak transmittance and on-state voltage is very important, since there might be variation on the cell gap during fabrication process. Figure 4 shows the T_p and V_{on} at different cell gap for both FFS-N1 and FFS-P1. The electrode width and gap are kept the same and λ=550nm is used in the calculation. For FFS-N1, as the cell gap increases from 2.8 μm ($d\Delta n$=333 nm) to 3.5 μm ($d\Delta n$=417 nm), V_{on} decreases slightly from 4.7V to 4.5V and T_p only varies by ~2%. That means, both V_{on} and T_p are insensitive to the cell gap variation, which is favorable from fabrication viewpoint. By contrast, in the same range the V_{on} of FFS-P1 rises almost linearly from 4.0V to 4.9V and T_p also increases from 82.4% to 91.8%.

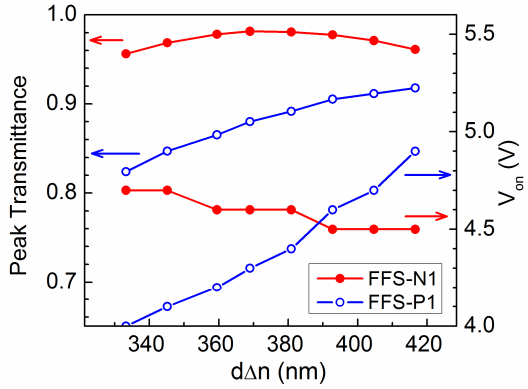

Figure 4. Cell gap effects on V_{on} and T_p of FFS-N1 and FFS-P1. λ=550 nm.

3.5. Viewing Angle

We also compare the viewing angle for the FFS cells using both positive and negative $\Delta\varepsilon$ LCs. Figure 5 shows the isocontrast plot for FFS-N1. The viewing angle properties of FFS-P1 (not shown here) is similar to that of FFS-N1, since their dark states are similar due to the same alignment and the contrast ratio (CR) difference is mainly determined by the bright state. FFS-N1 has a slightly better isocontrast performance because of its higher transmittance and more uniform in-plane director twist and small tilt angle in the bright state. To widen the viewing angle, various compensation films for FFS mode have been developed [17, 18]. With one biaxial film, a CR over 100:1 can be achieved in almost the entire viewing zone (±80°). To further widen the viewing angle, multi-domain structures can be considered [3].

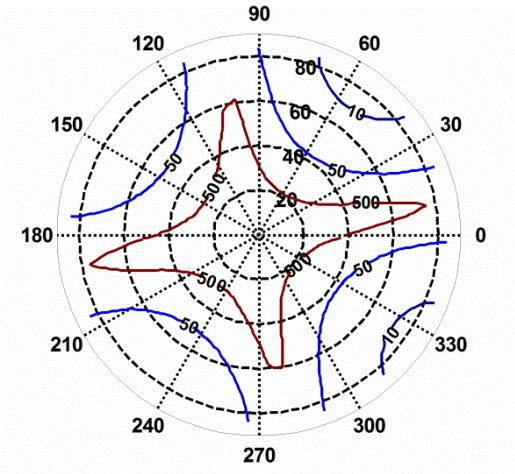

Figure 5. Simulated isocontrast plot for FFS-N1.

4. Conclusions

We have demonstrated a new negative $\Delta\varepsilon$ LC mixture with modest birefringence and low viscosity for FFS LCD. Our n-FFS shows superior performances to p-FFS in following aspects: 1) higher transmittance (98% vs. 88%); 2) single gamma curve for RGB pixels; 3) both on-state voltage and peak transmittance are insensitive to cell gap variation, 4) slightly wider viewing angle; 5) faster response time due to a slightly thinner cell gap and more efficient switching, and 6) comparable on-state voltage to p-FFS although the LC mixture has a smaller dielectric anisotropy ($\Delta\varepsilon\sim$ -3.8 vs. +10). Therefore, n-FFS has potential to replace p-FFS for next-generation mobile displays.

5. Acknowledgements

The authors are indebted to Dr. C. D. Tu for helpful discussion and Air Force Office of Scientific Research (AFOSR) under Contract FA95550-09-1-0170 for partial financial support.

6. References

[1] S. H. Lee, S. L. Lee, and H. Y. Kim, "Electro-Optic Characteristics and Switching Principle of a Nematic Liquid Crystal Cell Controlled by Fringe-Field Switching," Appl. Phys. Lett. **73**, 2881-2883 (1998).

[2] S. H. Lee, S. L. Lee, H. Y. Kim, and T. Y. Eom, "A Novel Wide-Viewing-Angle Technology: Ultra-Trans View," SID Symposium Digest, **30**, 202-205, (1999).

[3] S. H. Lee, S. M. Lee, H. Y. Kim, J. M. Kim, S. H. Hong, Y. H. Jeong, C. H. Park, Y. J. Choi, J. Y. Lee, and J. W. Koh, "18.1″ Ultra-FFS TFT-LCD with Super Image Quality and Fast Response Time," SID Symposium Digest, **32**, 484-487, (2001).

[4] J. B. Park, H. Y. Kim, Y. H. Jeong, D. H. Lim, S. Y. Kim, and Y. J. Lim, "Novel transflective fringe-field switching mode using common electrode with box and slit shape," Japanese Journal of Applied Physics Part 1-Regular Papers Brief Communications & Review Papers **44**, 6701-6702 (2005).

[5] S. H. Hong, I. C. Park, H. Y. Kim, and S. H. Lee, "Electro-Optic Characteristic of Fringe-Field Switching Mode Depending on Rubbing Direction," Jpn. J. Appl. Phys. **39**, L527-L530 (2000).

[6] M. Hird, "Fluorinated liquid crystals - properties and applications," Chem. Soc. Rev. **36**, 2070-2095 (2007).

[7] Y. Chen, Z. Luo, F. Peng, and S. T. Wu, "Fringe-Field Switching with a Negative Dielectric Anisotropy Liquid Crystal," J. Display Technol. **9**, 74-77 (2013).

[8] S. T. Wu, "Birefringence Dispersions of Liquid-Crystals," Phys. Rev. A **33**, 1270-1274 (1986).

[9] A. Lien, "Extended Jones Matrix Representation for the Twisted Nematic Liquid-Crystal Display at Oblique-Incidence," Appl. Phys. Lett. **57**, 2767-2769 (1990).

[10] Z. Ge, T. X. Wu, X. Zhu, and S. T. Wu, "Reflective liquid-crystal displays with asymmetric incident and exit angles," J. Opt. Soc. Am. A **22**, 966-977 (2005).

[11] Z. Ge, S. T. Wu, S. S. Kim, J. W. Park, and S. H. Lee, "Thin Cell Fringe-Field-Switching Liquid Crystal Display with a Chiral Dopant," Appl. Phys. Lett. **92**, 181109 (2008).

[12] H. J. Yun, M. H. Jo, I. W. Jang, S. H. Lee, S. H. Ahn, and H. J. Hur, "Achieving High Light Efficiency and Fast Response Time in Fringe Field Switching Mode Using a Liquid Crystal with Negative Dielectric Anisotropy," Liq. Cryst. **39**, 1141-1148 (2012).

[13] I. H. Yu, I. S. Song, J. Y. Lee, and S. H. Lee, "Intensifying the Density of a Horizontal Electric Field to Improve Light Efficiency in a Fringe-Field Switching Liquid Crystal Display," J. Phys. D: Appl. Phys. **39**, 2367-2372 (2006).

[14] J. W. Park, Y. J. Ahn, J. H. Jung, S. H. Lee, R. Lu, H. Y. Kim, and S. T. Wu, "Liquid crystal display using combined fringe and in-plane electric fields," Appl. Phys. Lett. **93**, 081103 (2008).

[15] L. M. Blinov and V. G. Chigrinov, *Electrooptic Effects in Liquid Crystal Materials* (John Wiley & Sons Ltd., New York, 1994).

[16] M. Jiao, Z. Ge, Q. Song, and S. T. Wu, "Alignment Layer Effects on Thin Liquid Crystal Cells," Appl. Phys. Lett. **92**, 061102 (2008).

[17] X. Zhu, Z. Ge, and S. T. Wu, "Analytical Solutions for Uniaxial-Film-Compensated Wide-View Liquid Crystal Displays," J. Display Technol. **2**, 2-20 (2006).

[18] R. B. Lu, X. Zhu, S. T. Wu, Q. Hong, and T. X. Wu, "Ultrawide-View Liquid Crystal Displays," J. Display Technol. **1**, 3-14 (2005).